

On Collapses in Strong Reversed Shear Plasmas During or Just After Plasma Current Ramp-Up in JT-60U

Takahiro BANDO^{a)}, Hiroshi TOJO, Manabu TAKECHI, Nobuyuki AIBA,
Takuma WAKATSUKI, Maiko YOSHIDA, Shizuo INOUE and Go MATSUNAGA
National Institutes for Quantum and Radiological Science and Technology, Naka, Ibaraki 311-0193, Japan

(Received 19 March 2021 / Accepted 25 May 2021)

The advanced tokamak (AT) scenario with the strong reversed magnetic shear is an attractive candidate of the steady state tokamak because the strong internal transport barrier leads to the high bootstrap current fraction, resulting in the reduction of the cost of the fusion reactor. In this paper, the causes of the collapses during or just after plasma current ramp-up of the experimental campaign of the AT scenario [Y. Sakamoto *et al.*, Nucl. Fusion **49**, 095017 (2009)] in 2007 and 2008 are investigated and the initial results are reported. As the observations are consistent with characteristics of the stability on the resistive wall mode (RWM) and the results of MARG2D code, the RWM is suggested as the candidate of the cause of the collapses in the analyzed AT scenario.

© 2021 The Japan Society of Plasma Science and Nuclear Fusion Research

Keywords: advanced tokamak scenario, strong reversed magnetic shear, collapse, resistive wall mode, JT-60U, tokamak

DOI: 10.1585/pfr.16.1402089

1. Introduction

The advanced tokamak (AT) scenario [1–11] with the strong reversed magnetic shear is an attractive candidate of the steady state tokamak because the strong internal transport barrier (ITB) [12] leads to the high bootstrap current fraction f_{BS} , resulting in the reduction of the cost of the fusion reactor. On the other hand, it is well known that many kinds of MHD instabilities [1–11] can occur in plasmas with the strong pressure gradient of ITB and the reversed magnetic shear, such as double tearing mode [2], locked tearing mode [4], resistive interchange mode [9], and resistive wall mode (RWM) [8, 13].

In JT-60U tokamak [14], which is one of pioneers to investigate the AT scenario, high f_{BS} plasmas with the reversed magnetic shear plasmas were developed between 2005 and 2008 with the plasma current $I_p \sim 0.8$ MA [7, 8]. In experimental campaign of 2005 and 2006 [7], the magnitude of the toroidal magnetic field, B_t , is greater than 3 T and the collapse hardly occurred with high injection power of neutral beam injections (NBI) ~ 15 MW during or just after plasma current ramp-up. On the other hand, in experimental campaign in 2007 and 2008 [8] with $B_t < 3$ T for smaller q_{95} scenario to the fusion reactor, the collapses occurred frequently even if the small injection power ~ 6 MW was applied by NBIs. The collapse rate, defined as the number of the discharge with the collapse to the number of the discharge, are summarized in Table 1 on the experimental campaign of the AT scenario between 2005 and 2008 [7, 8]. Here, the collapse until 4.8 s is in-

Table 1 Dependence of the collapse rate (indicated as “collapses/discharges”) until 4.8 s on the magnitude of the toroidal magnetic field B_t . The collapse rate increases as the decrease of B_t .

B_t	collapses/discharges
1.75T < B_t < 1.9T	13/18 \sim 72%
1.9 T < B_t < 2.2T	9/21 \sim 42%
2.2 T < B_t < 2.4T	3/53 \sim 5.6%
2.4 T < B_t < 2.9T	1/14 \sim 7.1%
3.0 T < B_t < 3.6T	5/184 \sim 2.7%

vestigated where the current ramp-up phase is generally finished. In the previous study on the campaign in 2007 and 2008 [8], the RWM is identified as the MHD mode to induce collapse in the current flat-top phase. However, the cause of collapses during or just after the plasma current ramp-up with smaller beta values than that in the flat-top phase has not been investigated. For further developments of the AT scenario, the cause of collapses in the experimental campaign in 2007 and 2008 should be investigated and the initial analytical results are reported in this paper.

2. Results of Analyses on Collapses

In the analyzed discharges in experimental campaign of 2007 and 2008 [8], $n = 1$ magnetic fluctuation is usually

author's e-mail: bando.takahiro.pd@tut.jp

^{a)} Present affiliation: Toyohashi University of Technology, Toyohashi, Aichi 441-8580, Japan

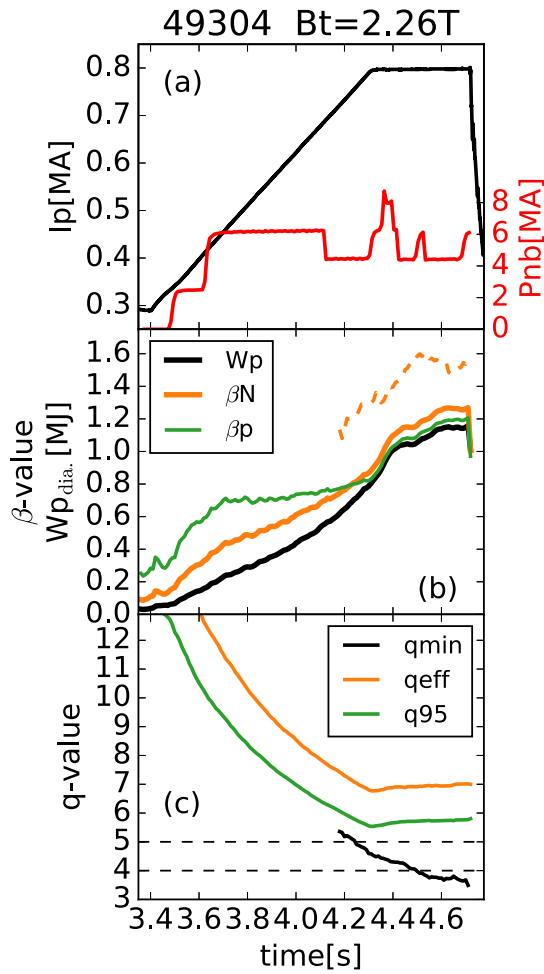


Fig. 1 Time evolution of (a) the plasma current and the injection power of P-NBIs (red line), (b) the plasma stored energy W_p , the normalized beta value β_N (orange line), and the poloidal beta value β_p (green line), and (c) the minimum of the safety factor profile q_{\min} , q_{eff} (orange line) [10], and q_{95} (green line). In (b), the orange dashed line is three times of the internal inductance $3\bar{l}_i(3)$. The definition of $\bar{l}_i(3)$ can be found in [15].

observed as the precursor of the collapse. In this paper, n and m are the toroidal mode number and the poloidal mode number, respectively. Figure 1 shows an example of the discharge with a collapse having the $n = 1$ precursor. As explained in [1], the reversed shear plasma is obtained with the heating during the current ramp-up as seen in Fig. 1 with the injection power of NBI ~ 6 MW. In this discharge, the collapse occurs around 4.7 s with the $n = 1$ precursor which grows with $\sim 800 \mu\text{s}$. The precursors are also observed in electron cyclotron emission (ECE) measurement. The growth time, which is greater than the Alfvén time scale [9], suggests the excitation of the RWM [8, 13]. In this study, the possibility of the RWM is investigated with MARG2D code [16] using the MHD equilibrium by the motional Stark effect measurement [17] and MEUDAS code [18]. Figure 2 (a) shows the safety factor (q) profile showing the strong reversed shear at 4.7 s of

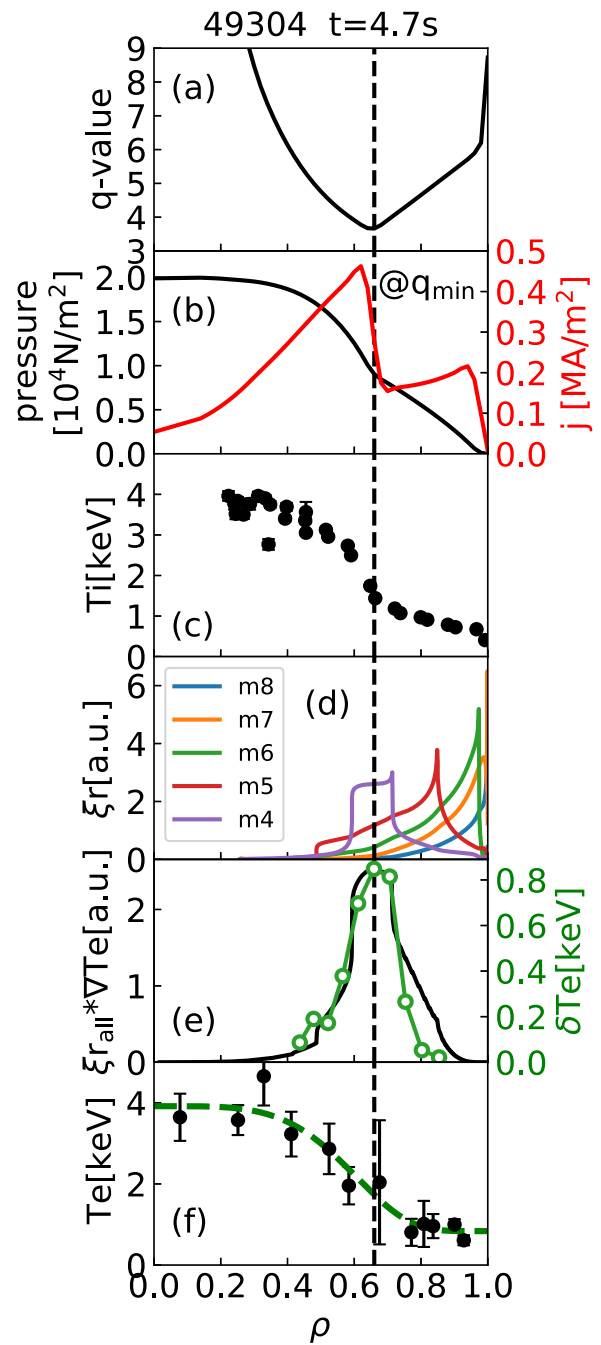


Fig. 2 Radial profiles of (a) the q -value, (b) the pressure and the plasma current (red line) of the equilibrium by MEUDAS code, (c) the ion temperature measured by charge exchange recombination spectroscopy (CXRS) measurement [19], (d) the ξ_r profile of the poloidal number $m = 4, 5, 6, 7,$ and 8 , (e) the comparison between δT_e and $\xi_{r,\text{all}} \times \nabla T_e$, and (f) the electron temperature profile with the green fitted curve measured by Thomson scattering measurement. The ρ is the normalized minor radius. The vertical dashed black line indicates the normalized minor radius at q_{\min} . In (d), the poloidal components, $m = 4, 5, 6, 7,$ and 8 , have the five highest amplitudes of ξ_r . In (e), $\xi_{r,\text{all}}$ is the sum of all poloidal components (29 poloidal components) of ξ_r . The summation of all poloidal components with a toroidal mode number is valid if the poloidal rotation velocity is damped, which is expected in tokamaks [20].

Table 2 Global plasma parameters at 4.7 s of 49304.

β_N	1.26 % m T MA ⁻¹
β_p	1.2
Plasma current	0.8 MA
Toroidal magnetic field	2.26 T
Major radius	3.5 m
Minor radius	0.94 m
Plasma volume	76 m ³
Plasma triangularity	0.4
Plasma elongation	1.4
q_{95} (the safety factor on 95% of flux surface)	5.76
q_{eff}	7.0
Plasma-wall separation in low field side	0.14 m

Fig. 1. The global plasma parameters at 4.7 s of 49304 are shown in Table 2. The peaked plasma current around the minimum of the safety factor profile, q_{min} , on the ITB in Figs. 2 (a) ~ (c) are consistent with the previous study [8]. The radial displacement, ξ_r , of the $n = 1$ mode estimated by MARG2D is shown in Fig. 2 (d). In Fig. 2 (e), the fluctuation of the electron temperature δT_e with the precursor is compared with $\xi_{r,\text{all}} \times \nabla T_e$. Here, $\xi_{r,\text{all}}$ is the sum of all poloidal components (29 poloidal components) of ξ_r . ∇T_e is the radial derivative of the electron temperature profile. δT_e is the difference of the electron temperatures at 4.716 s and 4.71864 s as shown in Fig. 3. Because MARG2D calculates the stability of the linear phase, the fluctuation component of the electron temperature is obtained at the peak indicated by the vertical dotted-dashed red line in Fig. 3. The decreased electron temperature after the vertical dotted-dashed red line is not used because the decreased temperature may be in the non-linear phase. The coincidence of the shape of the profile between δT_e and $\xi_{r,\text{all}} \times \nabla T_e$ indicates that the observed precursor in the electron temperature is due to the $n = 1$ RWM. In addition, in the case of Fig. 2, it is observed that the $n = 1$ mode is unstable without the ideal wall and the $n = 1$ mode is stable with the ideal wall, which is consistent with the characteristics of the stability of the RWM. As explained above, the $n = 1$ fluctuation observed just before the collapse is identified as the RWM because (a) the radial profile of the observed fluctuation is consistent with a theoretical prediction and (b) the theoretical predicted instability has the typical characteristics of the RWM, which is unstable (stable) without (with) the ideal wall.

Figure 4 presents another evidence of the excitation

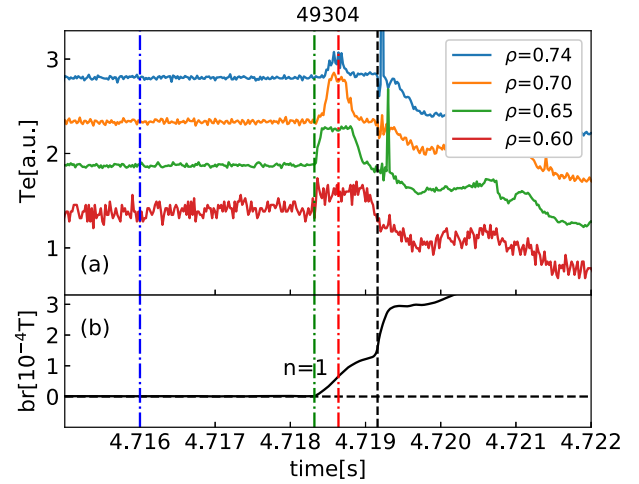


Fig. 3 Time evolution of (a) the electron temperature by ECE measurements from $\rho = 0.6, 0.65, 0.7$ and 0.74 and (b) the magnetic fluctuation. δT_e in Fig. 2 (e) is the difference of the electron temperatures between 4.716 s (vertical dotted-dashed blue line) and 4.71864 s (vertical dotted-dashed red line). The $n = 1$ mode starts to grow at 4.71832 s (vertical dotted-dashed green line). The collapse occurs at 4.71916 s (vertical dashed black line).

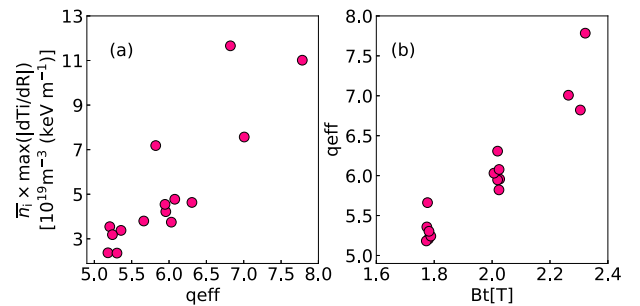


Fig. 4 (a) Relationship between q_{eff} and the maximum of the ion pressure gradient profile just before the collapse occurs. The ion density is calculated from the line-averaged electron density obtained with FIR measurement, the measured line-averaged effective ion charge, and the condition of quasineutrality. The included impurity in the plasma is assumed to be Carbon ($Z = 6$) only. The ion temperature profile is obtained with CXRS measurement [19]. (b) Relationship of q_{eff} and B_t where $I_p = 0.73 \text{ MA} \sim 0.8 \text{ MA}$. The dataset used in (a) and (b) is obtained from 15 discharges.

of the RWM. Figure 4 (a) shows a relationship of q_{eff} and the maximum of the absolute values of the ion pressure gradient profile just before the collapses occur. In the dataset of Fig. 4, I_p is $0.73 \text{ MA} \sim 0.8 \text{ MA}$. And the difference of q_{eff} comes from the difference of B_t as shown in Fig. 4 (b). In the analyzed reversed shear plasmas during or just after the current ramp-up, the plasma current may be accumulated in the edge region. And the edge plasma current has more destabilizing effect with smaller q_{eff} when the values of the plasma current are similar. As

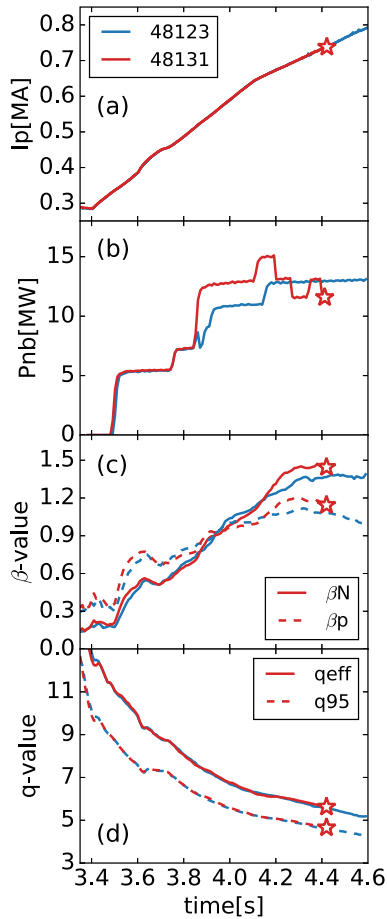


Fig. 5 Time evolution of (a) the plasma current, (b) the injection power of P-NBIs, (c) the normalized beta value β_N (solid line) and the poloidal beta value β_p (dashed line), and (d) q_{eff} (solid line) and q_{95} (dashed line). The red color and the blue color indicate the case with collapse (48131) and the case without the collapse (48123), respectively. In the case of the collapse, the collapse occurs at 4.42 s as indicated by the red markers.

mentioned above, the plasma current in the dataset is similar ($I_p = 0.73 \text{ MA} \sim 0.8 \text{ MA}$). Therefore, the dependence, smaller pressure gradient with smaller q_{eff} in Fig. 4 (a), can be interpreted as the smaller q_{eff} with larger destabilization effect by the edge plasma current limits the pressure gradient, which is the characteristics of the stability of the RWM [13]. The interpretation also suggests that the high collapse rate in the campaign at 2007 and 2008 of table 1 comes from the decreased limit of the pressure gradient with smaller q_{eff} (q_{95}) by smaller B_t .

In addition, if pairs of two discharges with and without the collapse having similar magnetic configurations and the heating power are compared, the case with higher normalized beta β_N or higher poloidal beta β_p shows the collapse at each pair. Figure 5 shows an example of the comparison between the case with the collapse 48131 and the case without the collapse 48123. In both discharges, $B_t \sim 1.77 \text{ T}$. The case with the collapse has the higher beta

values when the collapse occurs.

From above discussions, it is reasonable to suppose that the RWM induces the observed collapses during or just after the current ramp-up in the analyzed AT scenario.

3. Discussion and Future Study

In this paper, it is suggested that the RWM induces collapses during or just after the current ramp-up in JT-60U on the experimental campaign of the AT scenario at 2007 and 2008 [8]. In the previous study [8] on the analyzed campaign, it is suggested that the RWM was excited with $\beta_N > \beta_{N(\text{no-wall})} \sim 3li \sim 1.9$. Here, $\beta_{N(\text{no-wall})}$ is the normalized beta limit where the ideal MHD mode is destabilized without the ideal wall. li is the internal inductance and $3li$ is a measure of $\beta_{N(\text{no-wall})}$ in JT-60U [8]. However, in this study, β_N just before the collapse of Fig. 1 is 1.26 and is significantly smaller than $3li$ shown in Fig. 1 (b). The smaller β_N with the collapse in this study compared with that in the previous study on the current flat-top phase [8] may come from the accumulation of the plasma current around the edge region in the current ramp-up phase resulting in the larger destabilization effect by the plasma current. The larger destabilizing effect by the plasma current in the edge region allows the RWM mode to excite with the smaller pressure (β_N). Our results indicate that the RWM can occur with the smaller β_N than that reported in [8] even if $\beta_N < 3li$.

On the other hand, further analysis of the stability of the $n = 1$ RWM is still required. For example, the integer q_{min} passed many times in the current ramp-up phase (see Fig. 1 (c)). It may have destabilization effect on the RWM mode [7]. In addition, because MARG2D evaluates the stability with the pressure profile and the current profile excluding the stabilizing effect of the finite toroidal rotation velocity on the RWM [8, 13, 21], investigations of the stabilizing effect by the toroidal rotation velocity are also required with numerical codes such as MINERVA code [22] to evaluate and predict the stability of the RWM in the plasma current ramp-up phase of the AT scenario.

Acknowledgments

Helpful comments for analysis by Dr. Y. Sakamoto, Dr. N. Oyama, Dr. S. Ide, Dr. A. Isayama, Dr. T. Nakano, and F. Kin are greatly appreciated. The authors would like to thank Dr. A. Terakado on the re-evaluation of the data from CXRS measurement.

This work was supported by JSPS KAKENHI Grant Number JP18K03592.

- [1] R.J. Goldston, Phys. Plasmas **3**, 1794 (1996).
- [2] M. Kikuchi and M. Azumi, Rev. Mod. Phys. **84**, 1807 (2012).
- [3] T. Liu *et al.*, Nucl. Fusion **59**, 065009 (2017).
- [4] J.M. Hanson *et al.*, Nucl. Fusion **57**, 056009 (2017).
- [5] Y. Shen *et al.*, Nucl. Fusion **60**, 124001 (2020).

- [6] J. Huang *et al.*, Nucl. Fusion **60**, 126007 (2020).
- [7] Y. Sakamoto *et al.*, Nucl. Fusion **47**, 1506 (2007).
- [8] Y. Sakamoto *et al.*, Nucl. Fusion **49**, 095017 (2009).
- [9] S. Takeji *et al.*, Nucl. Fusion **42**, 5 (2002).
- [10] M. Takechi *et al.*, Nucl. Fusion **45**, 1694 (2005).
- [11] M. Takechi *et al.*, the 32nd EPS Conference on Plasma Physics (Spain, 27 June - 1 July 2005) P2.049.
- [12] K. Ida and T. Fujita, Plasma Phys. Control. Fusion **60**, 033001 (2018).
- [13] M.S. Chu and M. Okabayashi, Plasma Phys. Control. Fusion **52**, 123001 (2010).
- [14] N. Oyama and the JT-60 Team, Nucl. Fusion **49**, 104007 (2009).
- [15] G.L. Jackson *et al.*, Nucl. Fusion **48**, 125002 (2008).
- [16] N. Aiba *et al.*, Comput. Phys. Commun. **175**, 269 (2006).
- [17] T. Suzuki *et al.*, Rev. Sci. Instrum. **79**, 10F533 (2008).
- [18] M. Azumi, G. Kurita, T. Matsuura, T. Takeda, Y. Tanaka and T. Tsunematsu, Proc. of the 4th Int. Symp. on Computational Methods in Applied Science and Engineering (Paris, 1980) p.335.
- [19] M. Yoshida *et al.*, Fusion Eng. Des. **84**, 2206 (2009).
- [20] T.H. Stix, Phys. Fluids **16**, 1260 (1973).
- [21] M. Takechi *et al.*, Phys. Rev. Lett. **98**, 055002 (2007).
- [22] N. Aiba *et al.*, Comput. Phys. Commun. **180**, 1282 (2009).